

## Nanoliter Reactor Arrays for Antibiotic Study

Jin-Won Park

Gachon Bionano Research Institute, Kyungwon University, Kyungki 461-701, Korea. E-mail: jwpark@kyungwon.ac.kr

Received May 30, 2007

It is demonstrated in this study that the nanoliter reactor arrays with an inkjet printing, can be used for high throughput screen of antibiotic function. As a model antibiotic, gramicidin was used in this study. The gramicidin embedded lipid vesicles were immobilized on the surface in the nanoliter reactor structure with control of the volume in the nanoliter reactor. By dispensing acidic drops into the reactor, the gramicidin function was monitored. The technique developed in this research also has a great potential to be used for discovery of drugs.

**Key Words :** Nanoliter, Reactor, Arrays, Vesicles, Gramicidin

### Introduction

The study of the antibiotic reaction against bacteria requires reactions at numerous conditions. However, the reactions can be carried out with the proteins obtained through isolation and purification, which are difficult and time-consuming to be achieved. An amount of the proteins in a cell membrane is mostly  $\mu\text{M}$  scale, and the yield of the proteins is around 1%.<sup>1-3</sup> These facts lead to development of high throughput technologies. High throughput screen was performed with microwell plates, which require more than couple microliter volumes of a solution for reactions.<sup>4</sup>

Microfabrication technologies have been widely used, for example, drug delivery system,<sup>5,6</sup> *in vivo* application,<sup>7,8</sup> and micro-total analysis system ( $\mu\text{-TAS}$ ).<sup>9</sup> The microfabrication technologies have been also adapted for high throughput identification of DNA (DNA microarrays) to facilitate investigation of biological mechanism, which is extremely complicated.<sup>10</sup> However, since the data obtained from DNA microarray experiments does not provide any direct information about the function of the gene product, microarray has been developed for high throughput determination of a protein function (Protein microarrays).<sup>11-14</sup> Still, the present protein microarray technologies have a limitation that all of proteins immobilized on a surface are exposed to an identical chemical environment. Induction of all of proteins to different chemical surrounds apparently leads the antibiotic function study and the drug discovery to be carried out much more efficiently, because reactions at a lot of conditions are necessary for them.

Each chemical surround to each protein can not be achieved without a well defined microstructure and a sufficient reagent delivery system under well controlled humidity. The well defined microstructure plays as reactors, which isolate a reagent at a desired place from other reagents at other places on a single surface and provide a place for numerous reactions to occur. The isolation needs a barrier to keep the reagent from any leakage. In this paper, the microstructure in an array is called nanoliter reactor array. The nanoliter reactor allows one reaction to consume reagent in a nanoliter

scale, which is 1000 times less than a volume necessary in the microwell plate. And the reagent delivery system was introduced to transfer a reagent to a reactor at an exact place with minimization of contamination. Inkjet printing is inexpensive, repeatable, flexible, and easy to transfer of picoliter reagents.<sup>15</sup> Inkjet printing applications in biotechnology have been utilized previously including for biosensor development, biochips, DNA arrays, DNA synthesis, microdeposition of active proteins on cellulose, and free-form fabrication techniques to create polymeric scaffolds.<sup>16-22</sup> Humidity control is essential so that denature of proteins and variance of reagent concentrations in the nanoliter reactor could be avoided.

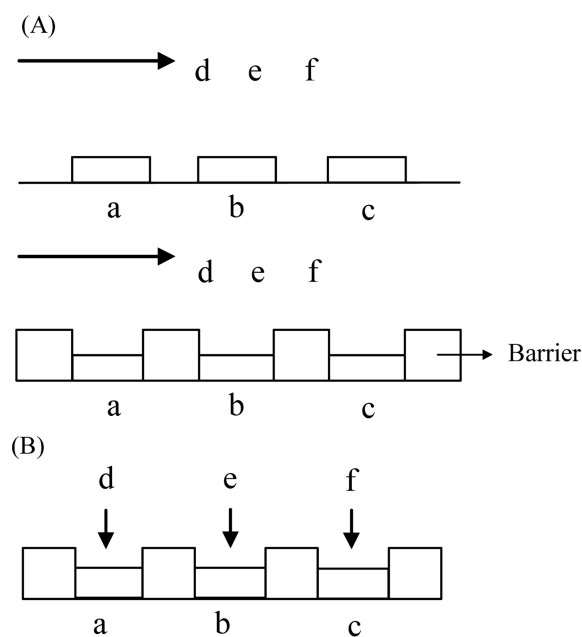


**Figure 1.** Schematic diagram to show the conventional protein arrays (A) and nanoliter reactor arrays (B). a, b, and c are corresponding to each protein, and d, e, and f are to each reagent reacted with the proteins. In (A), protein a, b, and c are exposed to all of reagents. In (B), each protein is exposed to a single reagent delivered using inkjet printing.

The goal of this study is to demonstrate that the nanoliter reactor arrays can be used with the inkjet printing for functional screening of antibiotics. As an antibiotic model, gramicidin has been selected because gramicidin function has been studied as a simple ionophore. Figure 1 presents schematic diagram to show the conventional protein array (Figure 1(A)) and the nanoliter reactor array (Figure 1(B)) pursued in this paper.<sup>22-24</sup> In Figure 1, a, b, and c are corresponding to each protein, and d, e, and f are to each reagent reacted with the proteins. In Figure 1(A), protein a, b, and c are exposed to all of reagents. However, in Figure 1(B), each protein is exposed to a single reagent delivered using the inkjet printing.

### Experimental

**Nanoliter array development.** Structure of the nanoliter reactor arrays was created with SU-8, which is an epoxy-based negative photo-resist that is well known for its utility in creating high aspect ratio polymeric microdevices.<sup>23-27</sup> The nanoliter reactor arrays were fabricated on an 18 × 18 mm cover glass (VWR, West Chester, PA). The microfabrication process involved seven steps are spin coat, soft bake, expose, post expose bake, develop, and hard bake. To obtain maximum process reliability, residual materials were removed from the microcover glass using an ozone-cleaner (UVO cleaner, model 42, Jetlight Co., Irvine, CA) for 10 minutes. Spin coating of the SU-8 photoresist (MicroChem Corp., Newton, MA) was carried out on a headway spin coating device (Headway Research Inc, Garland, TX). Before spin coating, the microcover glass was baked at 90 °C for 15 minutes to ensure all residual moisture was removed. The microcover glass was then taped to a polymer coated paper template and placed on the vacuum chuck of the spin coater. The SU-8 spin coating was carried out at 1,500 RPMs for 50 second to create 20-40 micron thick films, as determine profilometry in post processing (Tencor Alpha Step 200 Profilometer, Milpitas, CA). After coating the microcover glass, the template was removed and the device was soft baked at 65 °C for 5 minutes and then 95 °C for 10 minutes on the PMC Dataplate<sup>®</sup> digital hot plate (Mode: 731, Barnstead/ThermoLyne, Dubuque, IA). The nanoliter reactor pattern was designed with IC station (Mentor Graphics Corporation, Wilsonville, OR).

**Preparation of dye entrapped lipid vesicles.** Potassium Chloride (KCl), chloroform, and glycerin were purchased from Mallinckrodt (Hazelwood, MO). Tricine, Mes, and pyranine were purchased from Sigma-Aldrich (St. Louis, MO). Dipalmitoylphosphatidylcholine (DPPC), biotinylated dipalmitoylphosphatidylethanolamine (bio-DPPE), Rhodamine labeled dipalmitoylphosphatidylethanolamine (Rho-DPPE), and pegylated dipalmitoylphosphatidylethanolamine (PEG-DPPE) were purchased from Avanti Polar Lipids (Alabaster, PA). Large-unilamellar-vesicles (LUVs) were prepared with 98% DPPC, 1% bio-DPPE, 0.7% Rho-DPPE, and 0.3% PEG-DPPE.<sup>28</sup> The lipids were well mixed in chloroform to a total lipid concentration of 10 mg/mL.

The glass surface of a vial was coated with these lipids by evaporation of the solvent under a stream of nitrogen (Inweld Corp., Indianapolis, IN) during vortexing. Traces of solvent were removed under vacuum for 3-4 hours. The lipids were resuspended in a solution of 20% glycerin and 80% water of 0.1 M KCl, 5 mM Tricine, 5 mM Mes, and 5 mM pyranine at the desired pHs. During the resuspension, the lipid concentration was adjusted to the desired. This solution was subjected to ten freeze-thaw cycles with thaw performed above 40 °C. After the freeze-thaw cycles, the lipids form multi-lamellar-vesicles (MLVs). The MLVs were transferred into an extruder (Sciema Technical Services, Richmond, BC) and extruded through a standard polycarbonate filter (Osmonic, Westborough, MA). The vesicles were extruded ten times through a 0.1 μm pore size double polycarbonate filter above 40 °C. After the extrusion the LUVs were obtained. Excess dye (pyranine) outside of the vesicles was removed from the solution by gel chromatography (GC) made by packing 100 g Sephadex G-25 (Amersham Biosciences, Uppsala, Sweden) in a 45 cm length and 2.5 cm diameter glass column (Ace Glass, Louisville, KY). The packed materials (Sephadex G-25) in the column were rinsed twice, prior to adding the lipid vesicle solution into the column, with the buffer without pyranine, which was used for vesicle preparation. Break through curves were obtained by monitoring the dye concentration of the eluent of the lipid vesicle solution at 450 nm with UV/VIS spectrometer Lambda EZ 210 (Perkin Elmer, Boston, MA) to find a condition where a solution without dyes outside of the vesicles can be collected. All of UV/VIS absorption scanning to the lipid vesicle solution was performed using the lipid solution without pyranine as a reference at each pH unless otherwise stated.

**Gramicidin embedded lipid vesicles.** Gramicidin, selected as the membrane peptide model, is a hydrophobic protein consisting of 15 amino acids in the sequence of Val-Gly-Ala-Leu-Ala-Val-Val-Val-Trp-Leu-Trp-Leu-Trp-Leu-Trp.<sup>29</sup> Numerous studies using planar membranes and liposomes have shown that the channel is a dimer of the peptide. The total length is about 30 Å and the outer and inner diameters are ~15 Å and 5 Å respectively. The hydrophobic side chains are all on the outside of the helix and hydrophilic peptide backbone carbonyls line the pore. At sufficiently high levels of incorporation (>5 mol %) gramicidin aggregates to form tubular structures and induces the formation of hexagonal H<sub>II</sub> phase in model membranes.<sup>30</sup> Gramicidin was purchased from Sigma-Aldrich. For preparation of gramicidin embedded vesicles, gramicidin molecules were dissolved in ethanol and mixed with the lipids resuspended in a solution of 20% glycerin and 80% water of 0.1 M KCl, 5 mM Tricine, 5 mM Mes, and 5 mM pyranine at pH 8.2. Excess pyranine was removed with the procedures described above. Gramicidin concentration was 10 μM in the resuspended solution. 3 mL vesicle solution with gramicidin was added into a fluorometer cell (Perkin Elmer, Boston, MA), and the solution at different pH was monitored using the fluorometer - Luminescence Spectrometer LS50B (Perkin Elmer, Boston, MA)

with 460 nm excitation and 520 nm emission wavelengths. Vesicle solution without gramicidin was also monitored in the same way.

**Surface chemistry.** Chemical treatment on a nanoliter reactor surface was performed to lead lipid vesicles to bind to the surface. Biotin groups were necessary to be immobilized on the surface so that lipid vesicles made with biotinylated lipids could be bound to the surface through streptavidin molecules (Sigma-Aldrich, St. Louis, MO). The surface needs to provide not only a specific binding to the lipid vesicles but also resistance to non-specific adsorption of streptavidin molecules. Therefore, biotin attached polyethylene glycol (bio-PEG) was immobilized by reacting *N*-hydroxysuccinimide (NHS) ester PEGs (Nektar, San Carlos, CA) after nanoliter reactor surfaces were aminated by a process of adsorption of polyethyleneimine (PEI) (Sigma-Aldrich, St. Louis, MO). The surfaces were ozone-cleaned prior to the amination. All reactions were performed at room temperature unless otherwise stated. PEI with a mean molecular weight of 500,000 was adsorbed on the surfaces by incubation with 5% (w/v) PEI in 50 mM sodium carbonate ( $\text{Na}_2\text{CO}_3$ , Mallinckrodt, Hazelwood, MO), pH 8.4 for 1 hour. Excess PEI was removed by through rinsing in water. PEG derivatives were 20 mg/mL  $\alpha$ -biotin,  $\omega$ -NHS polyethylene carbonate, MW 3400. After thorough rinsing, the surfaces were dipped in a solution of 20  $\mu\text{g}/\text{mL}$  streptavidin concentrations in the PBS buffer for 1 hour. The nanoliter reactor surface was rinsed twice in 40 mM octylglucoside (Pierce Biotech, Rockford, IL) for 5 minutes and ten times in the 0.1 M potassium chloride (KCl), 5 mM Tricine, 5 mM Mes buffer at desired pH. After removal of non specific bound streptavidin molecules from the nanoliter reactor surface, the surfaces were ready for lipid vesicle immobilization on the nanoliter reactor surface. Lipid vesicle immobilization was performed through biotin-streptavidin specific binding for two different purposes, 1) to investigate whether the lipid vesicles immobilized on a surface were fused to form lipid bilayer, because the gramicidin in lipid bilayer also has the capability to exchange protons, and 2) to conduct a gramicidin function assay on the nanoliter reactor arrays. For all of two cases, the nanoliter reactor surface was incubated in 10 mM lipid vesicle solution for two hours. Explanation for all of experiments is following in detail.

**AFM measurements.** Nanometer scale images were obtained at each step of chemical treatment on a surface without the nanoliter reactor arrays, using the atomic force microscope (AFM). From the images, it is shown 1) that the lipid vesicles were immobilized on the surface through the specific binding (streptavidin-biotin) and 2) that the lipid vesicles were not fused to form lipid bilayer. The lipid vesicles prepared without gramicidin were immobilized on the surface in a solution of 20% glycerin and 80% water of the 0.1 M KCl, 5 mM Tricine, 5 mM Mes buffer at pH 8.2, and excess lipid vesicles were gently rinsed with the solution used for the incubation twice. Concerning effects of gramicidin to the immobilization and the fusion, the gramicidin embedded lipid vesicles were also immobilized on the

surface with the identical procedures described above.

**Gramicidin function assay.** The gramicidin embedded lipid vesicles were immobilized on the surface in a solution of 20% glycerin and 80% water of the 0.1 M KCl, 5 mM Tricine, 5 mM Mes buffer at pH 8.2, and excess lipid vesicles were gently rinsed with the solution used for the incubation twice. As a control, the lipid vesicles prepared without gramicidin were used with the identical procedures described above. Right after relative humidity reached to 100% in the humidity control chamber, the nanoliter reactor arrays were transferred on an optical microscope stage inside of the humidity control chamber. The vesicle solution on a SU-8 barrier between the reactors was swept with a cleaned glass slide, right before the relative humidity was adjusted to 95%. (Pure water was easily evaporated during the sweeping, because the relative humidity was lower while the water on the barrier was swept). Then, acid drops (pH 3) were dispensed to the nanoliter reactors using an inkjet printing (Microfab, Inc., Plano, TX). Fluorescence images were taken after 1 minute from the dispensation using the CoolsnapHQ monochrome camera (Fryer Company, Inc., Huntley, IL) whose quantum efficiency is over 60% at pyranine emission wavelength (520 nm).

## Results and Discussion

Nanoliter reactor arrays were shown in Figure 2, an optical micrograph of micro-reactors 400, 500 and 600 microns in diameter. Liquid volume in the reactor was controllable upon the relative humidity. Volume control in the nanoliter reactor is essential to keep a concentration of reagents constant so that quantitative data could be obtained for a reaction in the nanoliter reactor. Pure water is, as a solvent in the nanoliter reactor, not appropriate even at maximum relative humidity due to technical limitation, which is described in the gramicidin function assay section later. The volume was controlled with water-glycerin composition and relative humidity around the nanoliter reactor. It was observed that the volume was easier to be kept constant with pure glycerin, but in the pure glycerin diffusion of the reagent was found to be much slower diffusion of the reagent in the nanoliter reactor. Since 20% (w/w) of glycerin is known to be a composition which a viscosity is increased

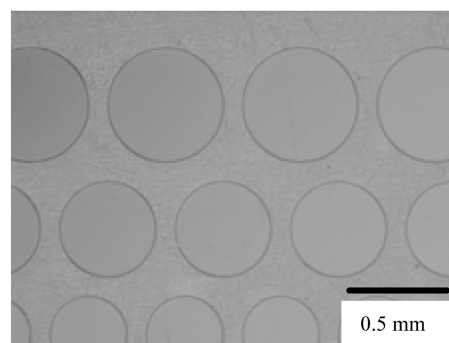


**Figure 2.** Optical micrograph of a nanoliter reactor array with reactors 400, 500, and 600 microns in diameter.

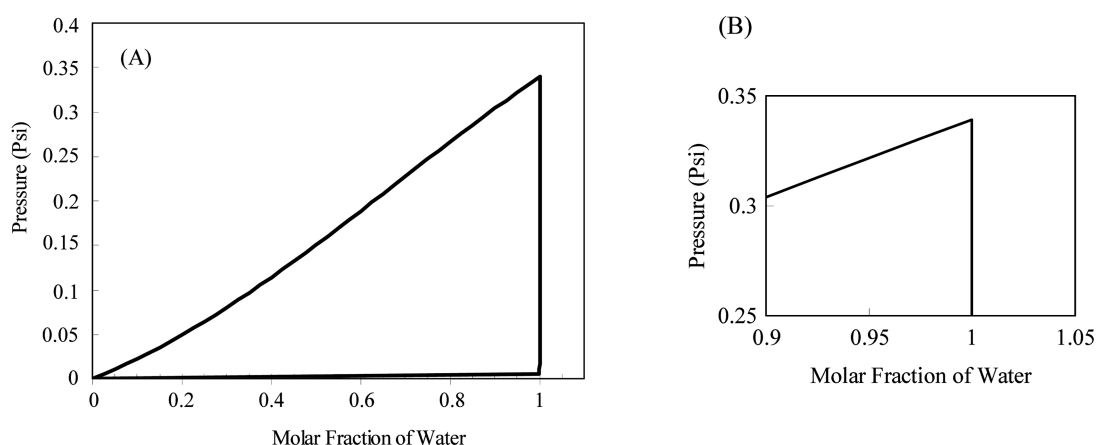


**Figure 3.** Phase diagram of water-glycerin. (A) phase diagram in a whole range of water molar fraction. (B) Magnification of the phase diagram around 0.95 water molar fraction.

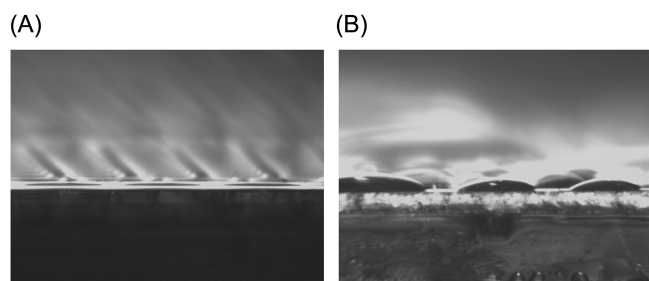


**Figure 4.** Volume Control on Microfabricated Reactor Arrays. (A) is at 95% relative humidity, and (B) is at least 100% more than 2 hours.

significantly above,<sup>31</sup> 20% (w/w) was chosen as a starting point. Diffusion is observed to become significantly slow at more than 20% (w/w) glycerin in aqueous solution. 20% (w/w) glycerin corresponds to 95% water molar fraction in aqueous solution, and a phase diagram of water and glycerin is found in terms of vapor pressure with respect to molar fraction of water using Aspen Plus<sup>®</sup>. The phase diagram in Figure 3 suggests that vapor pressure of 95% water molar fraction in liquid phase is identical with that of 95% relative humidity in vapor phase.

The result of theoretical simulation above was found consistent with the experimental observation. Figure 4 presents solution-air interfaces at different relative humidity condition. Figure 4(A) shows that the interface is almost flat at 95% relative humidity. Figure 4(B) shows that the interface is convex when the relative humidity was kept at 100% relative humidity for at least more than 2 hours. Once relative humidity in the chamber was kept around 95% relative humidity, no net change in the volume of the liquid in the reactor is observed. Therefore, it is concluded that a concentration of reagents in the nanoliter reactor is not changed at 95% relative humidity after the reagents are transferred from the inkjet printing head to the nanoliter reactor. The increased amount of volume from keeping relative humidity of 100% for 2 hours could be estimated using the optical image in Figure 4(B). The increased amount is about 9 nanoliter, which is almost identical with

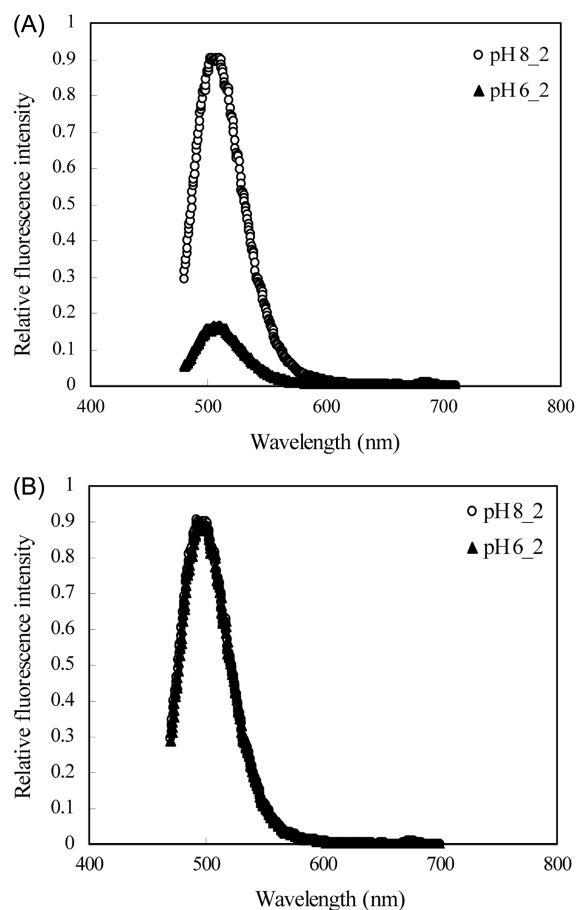


**Figure 5.** pH-Dependent Change in Fluorescence Intensity of Pyranine Entrapped within Lipid Vesicles in the Presence of Gramicidin (A) and in the Absence of Gramicidin (B). Excitation wavelength is 450 nm, and emission wavelength is 510 nm.

the volume of the nanoliter reactor which has 600 micron diameter and 30 micron depth, 8.5 nanoliter. Therefore, the volume variation can induce two times less than the concentration at 95% relative humidity.

Fluorescence intensity of the vesicle solution was measured at pH 8.2. After acid drops (pH 3) were added to

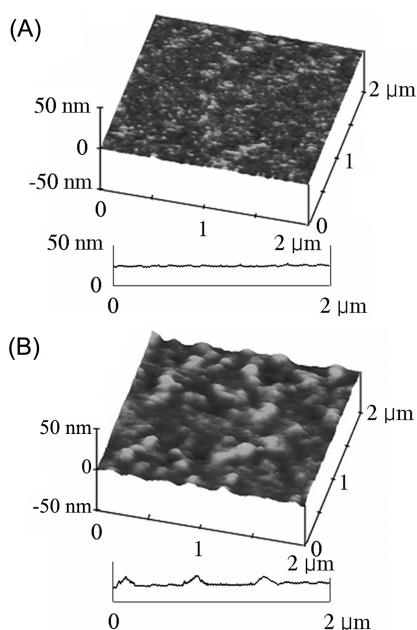


**Figure 6.** AFM images. (A) Morphology of the surface before the lipid vesicles were immobilized. (B) Morphology of the surface after the lipid vesicles were immobilized.

convert pH 8.2 into pH 6.2 in the solution, fluorescence intensity was measured again. Peak change in a fluorometer spectrum is monitored. At the lipid vesicle solution with gramicidin the peak change is observed, while it is not at the lipid vesicle without gramicidin (Figure 5). This observation could be explained with a function of gramicidin embedded in the lipid vesicles. The function could be considered as a channel which protons are exchanged through. A known permeability of protons across the lipid bilayer is much less than that of gramicidin.<sup>32</sup> It is also known that proton gradient does not cause osmotic pressure across the lipid bilayer,<sup>33</sup> whose agreement is shown with the observation of no fluorescence intensity change at the lipid vesicle solution without gramicidin. Pyranine has been found to be a reliable and convenient probe of the pH of the internal aqueous compartment of phospholipid vesicles. It is observed that ionization of the 8-hydroxyl group of pyranine at alkaline

pH ( $pK_a = 7.2$ ) was associated with a pronounced red shift in the fluorescence excitation maximum from 400 (pH 4) to 450 nm (pH 10), while the 510 nm emission maximum remained essentially unchanged.<sup>34</sup> Therefore, the amplitude of the 510 nm fluorescence excited at 450 nm reflects the concentration of the unprotonated species. Fluorescence intensity changes are monitored for pyranine entrapped lipid vesicles with gramicidin and without gramicidin at 450 nm excitation and 510 nm emission wavelength. Almost no fluorescence intensity is changed for lipid vesicles without gramicidin, while it is changed for lipid vesicles with gramicidin. Gramicidin works as an ion transport channel. It is known that water passes through a gramicidin channel at a permeability of about  $10^2$  cm/s, while the permeability of DPPC bilayer is about  $10^{-7}$  cm/s.<sup>35,36</sup> For the gramicidin embedded lipid vesicle solution, the fluorescence intensity change up to pH change was analyzed quantitatively. The fluorescence intensity ratio at pH 6.2 to pH 8.2 was  $7 \pm 1\%$ , which is consistent with other article results.<sup>37</sup> This ratio is found almost identical with unprotonated pyranine molecule ratio of pH 6.2 to pH 8.2, which is 9.8%. The unprotonated pyranine molecule ratio was calculated using Henderson-Hasselbalch equation. 91% of pyranine molecules is unprotonated at pH 8.2 and 9% of pyranine molecules is unprotonated at pH 6.2.

In nanometer scale morphology, no significant difference from the embedded gramicidin was found. The AFM images were shown in Figure 6. PEI, biotinylated PEG, and streptavidin modified surface morphologies are observed almost identical. The image before the lipid vesicle immobilization is presented in Figure 6(A). In Figure 6(A), maximum step height is observed less than 2 nm, and cross section width of most morphological bumps is found less than 100 nm. This characteristic appears to be that of PEI surface, because morphologies of PEI, PEG, and streptavidin modified surfaces were almost identical. Figure 6(B) shows the image after the lipid vesicle immobilization. Step height reaches up to almost 10 nm and cross section width of most bumps are found around  $190 \pm 60$  nm, which is predictable because the lipid vesicle diameter was measured  $140 \pm 60$  nm using light scattering instrument Coulter N4 Plus Submicron Particle

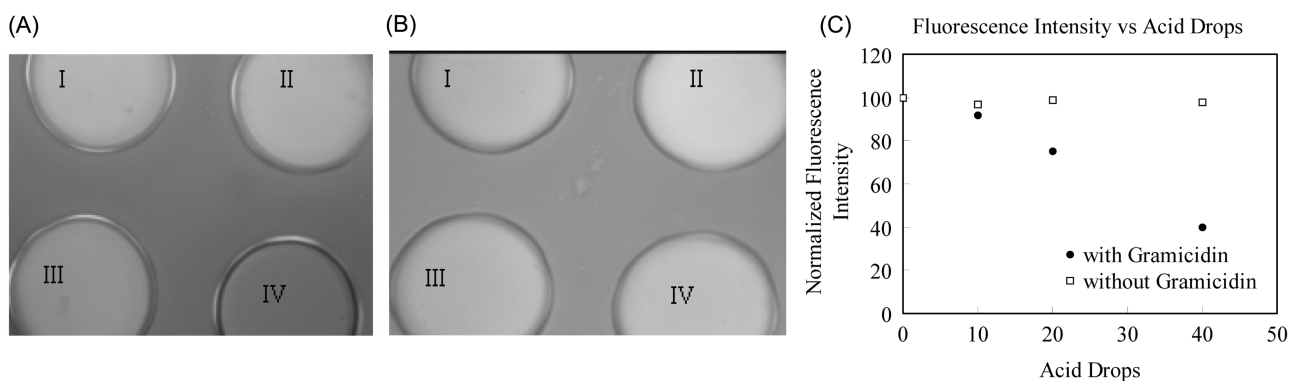


**Figure 7.** (A) Fluorescence image of a micro-fabricated reactor surface with lipid vesicles where gramicidin molecules were embedded. (B) Fluorescence image without gramicidin molecules. No acid drops (II), 10 acid drops (I), 20 acid drops (III), and 40 acid drops (IV). (C) Summary of Normalized Fluorescence Intensity Change for (A) and (B).

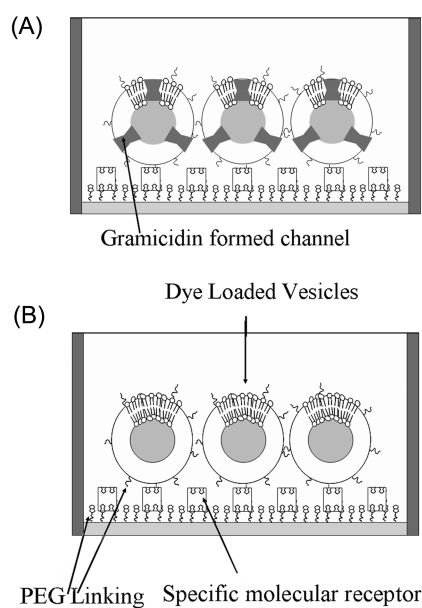


**Figure 8.** Schematic diagram of structure inside the nanoliter reactor. (A) The gramicidin embedded lipid vesicles were immobilized on the surface inside of the nanoliter reactor. (B) The immobilized lipid vesicles were prepared without gramicidin.

Sizer (Beckman Coulter, Fullerton, CA).

Fluorescence intensity decrease was observed upon gramicidin embedment, with pH decrease. Figure 7 shows the obtained images. Fluorescence image in Figure 7(A) is for the lipid vesicles prepared with gramicidin, and that in Figure 7(B) is for the lipid vesicles without gramicidin. It is observed that more added acid drops cause lower fluorescence intensity from I through to IV in Figure 7. Fluorescence intensities of Figure (A) and (B) were normalized with respect to the fluorescence intensity of no acid drop. The normalized data were summarized in Figure 7(C). It is obvious that the fluorescence intensity change was caused by protons exchanged through channels formed by gramicidin. To make points crystal clear, schematic diagram to show structures inside of the nanoliter reactor is presented in Figure 8. Apparently, the fluorescence changes in Figure 7(A) could be interpreted with the structure shown in Figure 8(A). Likewise, the results found in Figure 7(B) could be described with Figure 8(B).

In conclusion, it was demonstrated that the nanoliter reactor arrays can be used with the inkjet printing for functional screening of antibiotics. Furthermore, the technique developed in this research also has a great potential to be used for discovery of drugs.

**Acknowledgments.** This research was supported by Gachon Bio-Nano Research Institute, Kyungwon University. We thank the members of the Institute for valuable discussions.

## References

- Hamada, H.; Tsuruo, T. *J. Biol. Chem.* **1988**, *263*, 1454.
- Sousa, V. L.; Costa, M. T.; Palma, A. S.; Enguita, F.; Costa, J.

- Biochem. J.* **2001**, *357*, 803.
- Viard, M.; Blumenthal, R.; Raviv, Y. *Electrophoresis* **2002**, *23*, 1659.
- Brown, A. M.; George, S. M.; Blume, A. J.; Dushin, R. G.; Jacobsen, J. S.; Sonnenbergreines, J. *Anal. Biochem.* **1994**, *217*, 139.
- Santini, J. T.; Cima, M. J.; Langer, R. *Nature* **1999**, *397*, 335.
- Jackman, R. J.; Duffy, D. C.; Ostuni, E.; Willmore, N. D.; Whitesides, G. M. *Anal. Chem.* **1998**, *70*, 2280.
- Beebe, D. J.; Moore, J. S.; Bauer, J. M.; Yu, Q.; Liu, R. H.; Devadoss, D.; Jo, B.-H. *Nature* **2000**, *404*, 588.
- Service, R. F. *Science* **2002**, *297*, 962.
- Burns, M. A.; Johnson, B. N.; Brahmasandra, S. N.; Handique, K.; Webster, J. R.; Krishnan, M.; Sammarco, T. S.; Man, P. M.; Jones, D.; Heldsinger, D.; Mastrangelo, C. H.; Burke, D. T. *Science* **1998**, *282*, 484.
- Choi, Y. S.; Lee, K. S.; Park, D. H. *Bull. Korean Chem. Soc.* **2005**, *26*, 379.
- Stamou, D.; Duschl, C.; Delamarche, E.; Vogel, H. *Angew. Chem. Int. Ed.* **2003**, *42*, 5580.
- MacBeath, G.; Schreiber, S. L. *Science* **2000**, *289*, 1760.
- Zhu, H.; Klemic, J. F.; Chang, S.; Bertone, P.; Casamayor, A.; Klemic, K. G.; Smith, D.; Gerstein, M.; Reed, M. A.; Snyder, M. *Nat. Genet.* **2000**, *26*, 283.
- Michaud, G. A.; Salcius, M.; Zhou, F.; Bangham, R.; Bonin, J.; Guo, H.; Snyder, M.; Predki, P. F.; Schweitzer, B. I. *Nat. Biotechnol.* **2003**, *21*, 1509.
- Roth, E. A.; Xu, T.; Das, M.; Gregory, C.; Hickman, J. J.; Boland, T. *Biomaterials* **2004**, *25*, 3707.
- Newman, J. D.; Turner, A. P. F.; Marrazza, G. *Anal. Chim. Acta* **1992**, *262*, 13.
- Xu, T.; Petridou, S.; Lee, E. H.; Roth, E. A.; Vyavahare, N. R.; Hickman, J. J.; Boland, T. *Biotechnol. Bioeng.* **2004**, *85*, 29.
- Allain, L. R.; Askari, M.; Stokes, D. L.; Vo-Dinh, T.; Fresenius, J. *Anal. Chem.* **2001**, *371*, 146.
- Blanchard, A. P.; Kaiser, R. J.; Hood, L. E. *Biosens. Bioelectron.* **1996**, *11*, 687.
- Roda, A.; Guardigli, M.; Russo, C.; Pasini, P.; Baraldini, M. *Biotechniques* **2000**, *28*, 492.
- Sherwood, J. K.; Riley, S. L.; Palazzolo, R.; Brown, S. C.; Monkhouse, D. C.; Coates, M.; Griffith, L. G.; Landeen, L. K.; Ratcliffe, A. *Biomaterials* **2002**, *23*, 4739.
- Park, A.; Wu, B.; Griffith, L. G. *J. Biomater. Sci. Polym. Ed.* **1998**, *9*, 89.
- Lee, K. Y.; Labianca, N.; Rishton, S. A.; Zolgarain, S.; Gelorme, J. D.; Shaw, J.; Chang, T. H.-P. *J. Vac. Sci. Technol. B* **1995**, *13*, 3012.
- Shaw, J. M.; Gelorme, J. D.; Labianca, N. C.; Conley, W. E.; Holmes, S. J. *IBM J. Res. Dev.* **1997**, *41*, 81.
- Malek, C. G. K. *Microelectr. J.* **2002**, *33*, 101.
- Park, S. H.; Lim, T. W.; Yang, D. Y.; Kong, H. J.; Kim, R. H.; Kim, K. S.; Lee, K. S. *Bull. Korean Chem. Soc.* **2004**, *25*, 1119.
- Lee, J. H.; Woo, S. Y.; Kwon, Y. U.; Jung, D. Y. *Bull. Korean Chem. Soc.* **2003**, *24*, 183.
- Walde, P.; Ichikawa, S. *Biomol. Eng.* **2001**, *18*, 143.
- Sarges, R.; Witkop, B. *J. Am. Chem. Soc.* **1965**, *87*, 2011.
- Brasseur, R.; Killian, J. A.; de Kruijff, B.; Ruysschaert, J. M. *Biochim. Biophys. Acta* **1987**, *903*, 11.
- Zhang, X.; Padgett, R. S.; Basaran, O. A. *J. Fluid Mech.* **1996**, *329*, 207.
- Gennis, R. B. *Biomembranes: Molecular Structure and Function*; Springer-Verlag: New York, 1989; pp 288-290.
- New, R. R. C. *Liposomes a Practical Approach*; IRL Press: Oxford, U. K., 1990; pp 14-16.
- Kano, K.; Fendler, J. H. *Biochim. Biophys. Acta* **1978**, *509*, 289.
- Deamer, D. W. *J. Bioenerg. Biomembr.* **1987**, *19*, 457.
- Hladky, S. B.; Haydon, D. A. *Curr. Top. Membr. Trans.* **1984**, *21*, 327.
- Clement, N. R.; Gould, J. M. *Biochemistry* **1981**, *20*, 1534.